Hardware implementation of WPT Charging System for EV Vehicles

Srividya Devi P[1*], *Satya Narayana* Vemula[1], *Om* Pohanekar[1], *Rekha* Mudundi[1], *S*. Obad[2]

[1]Department of EEE, GRIET, Hyderabad, Telangana, India.
[2]Department of Refrigeration and air Conditioning Techniques engineering, College of technical engineering, The Islamic University, Najaf, Iraq.

Abstract. Transportation in urban areas is being transformed by various vehicles, with e-scooters being among the fastest growing. Despite their popularity, e-scooters face issues like incompatible chargers, especially problematic for rental services. Wireless charging emerges as a solution by enabling battery charging without user intervention. This paper focuses on the design and development of a magnetic-resonance charger for e-scooters. This research has detailed the coil topology, gap definition, and optimized control for a constant current-constant voltage (CC-CV) charge. This present key contribution is the integrated consideration of these factors, alongside the vehicle's materials and structure, for precise design and implementation. The vehicle's dimensions significantly constrain the coil design. Thus, in the past, a detailed analysis using Ansys Maxwell to determine the optimal locations for primary and secondary coils in an actual e-scooter was carried out. This analysis led to an optimal design for coil geometries, minimizing costs. The proposed system was validated with a real prototype, incorporating CC-CV control to ensure safe charging for various battery states, and is adaptable to a wide range of e-scooters, enhancing the usability of such chargers in public installations.

1 Introduction

Huge developments are happening in EVs with respect to battery charging wirelessly. Vast studies like pulse charging units, about Lithium-ion battery, their charging with the EVs is demonstrated [1-4]. And due to this various power quality issues exist on grid while EVs are on onboard charging [5-8]. Various materials are used based on the feasibility of the insulators, wide analysis on the usage of materials is carried using SEM type of equipment [9-10]. Various software is available for the modeling of inductors for the WPT system [11-14]. Using ANSYS software simulations to obtain the necessary results, this project is moved forward with actual calculations and development of a real-time working model. This project introduces a wireless power transmission system for electric vehicles (EVs) employing a detailed setup. On the transmission side, components such as a step-down transformer, rectifier, capacitive bank, MOSFET, Arduino UNO and copper coil are used to effectively transfer power wirelessly. Magnetic field created by the transmitter helps to produce current in the EV by induction process. On the other side the microcontroller is used to interact to produce the rectified current to operate on board. Here the transfer of power is done wirelessly. The main disadvantage of owning an EV is the minimal charging infrastructure in the urban environment. This last limitation restricts the

[*] Corresponding Author: srividyadevi.p@griet.ac.in

use of EVs. Wireless charging has emerged as a potential solution to the challenges faced by e-scooters, such as incompatible chargers. By allowing batteries to be charged without user intervention, wireless charging addresses these drawbacks and promotes the e-scooter revolution. However, the design process and implementation details of a magnetic-resonance charger for e-scooters require careful consideration.

2 Hardware Requirements

In order to build the hardware for charging the EV Vehicle with wireless power transmission (WPT) system their major specifications of the modules used.

1. Step down transformer 230v to 12volts, 5 amps.
2. Function generator ICs like (8038, 1458, xr2206)
3. Mosfet drivers.(irfz44, irf540,irf9140, irfp150)
4. Two copper coils.
5. PIC and Arduino UNO Microcontrollers.
6. LCD.
7. Capacitor bank.
8. Rectifier.

2.1 Step down Transformer:

A transformer is a static electromagnetic device that uses the magnetic field between its main and secondary windings to induce voltage. The primary side is where the 230-volt input is located. The transformer has a 5-volt (AC only) output. The step-down transformer and ratings of 0-12-0V were utilized in this Hardware experimentation.

2.2 Rectifiers and Filters:

Because an H bridge rectifier has a higher efficiency than any other rectifier, it is used in this project. This rectifier produces non-pure DC output. It might have some pulsating DC ripple components in it. Filters are employed to remove the ripple component that is present in the output circuit. In this circuit, the filter is employed to remove ripples from the rectified output. There are a variety of filter kinds. A capacitor filter is used by most of the power supply. Its purpose is to remove any ripples from the output. Any undesirable ripple or noise signal is filtered out by the capacitor that is employed as a filter at the input side following the solar panel.

2.3 MOSFETs:

The MOSFET, also known as the metal-oxide semiconductor field-effect transistor, is a type of transistor that is typically used for electrical signal switching and amplification. The MOSFET has four terminals: source (S), gate (G), drain (D), and body (B). However, like other field-effect transistors, it has three terminals because the body, also known as the substrate, is frequently linked to the source terminal. Electrical diagrams show only three terminals when two terminals are linked. Although the bipolar junction transistor was once significantly more prevalent, the MOSFET is by far the most used transistor in both digital and analogue circuitry.

2.4 Copper Coils:

A conductor, usually an insulated solid copper wire, is converted into an electromagnetic coil ("coil") when it is twisted around a core or formed into an electromagnet or inductor. A coil is made up of one or more turns, each of which is referred to as a turn of wire. Taps, which are electrical connection terminals, are linked to coils in electronic circuits. To offer extra insulation and keep coils in their proper functioning position, insulating tape or varnish coatings are frequently applied to them. A winding is a finished coil assembly that includes taps. The project employs coils based on the notion of a transformer, which is a stationary electromagnetic device with a primary winding and a secondary winding for the purpose of transferring energy from one

2.5 PIC Microcontroller (16F72):

Also referred to as a microcontroller for peripheral interface. Except the supply pins (4 pins), the PIC 16F72 is a 28-pin integrated circuit with 3 ports: port A (6 pins), port B (8 pins), and port C (8 pins). The PIC microcontroller in this project is utilized to operate circuits above 5V. The receiving side PIC microcontroller's connection diagram is displayed in Fig 5.

2.6 Arduino Uno:

The ATmega328 microprocessor board from the AVR family powers the Arduino Uno. This kind of microcontroller uses a reset button in addition to having six analogue pins, sixteen digital input and output pins, sixteen millimetre-wave ceramic resonators, a USB port, and a power jack. Programming is made easy by the multiple libraries that support its applications. The connection diagram for the hardware-based Arduino UNO pins is displayed in Figure 4. The Arduino UNO is utilised in this project to provide clock pulses to the H Bridge, increasing the frequency from 50Hz to 85KHz.

2.7 LED Indicators:

LEDs are used more often for general illumination applications and as indication lights in a variety of gadgets. LEDs used to emit low-intensity red light, but more recent models have very high brightness and can now emit light over the visible spectrum, as well as ultraviolet and infrared wavelengths. Compared to conventional indicators, LED indicators require 90% less electricity and have a minimum ten-year lifespan.

2.8 H Bridge Inverter:

This is one of the major parts in hardware implementation. The H-bridge circuit can be built as discrete components or integrated into an integrated circuit and is often used in inverters (DC-AC conversion).

2.9 LCD Display:

A liquid crystal display (LCD) is a thin, flat electronic visual display that uses the light-modulating properties of liquid crystals. LCD is a very important device in embedded systems. It offers high flexibility to the user as it can display the required data on it.

2.10 Voltage Sensor:

Voltage dividers are used for adjusting the level of a signal, for bias of active devices in amplifiers, and for measurement of voltages.

3 Transmission and receiving System design circuits

For designing a WPT circuit, it requires the transmission and receiving units for charging. In the previous WPT analysis, we used the ANSYS to design the primary coil and secondary coil. Figures 1 & 2 show the block diagram of the transmission unit and receiving units of the WPT circuit.

 https://doi.org/10.1051/e3sconf/202455201148

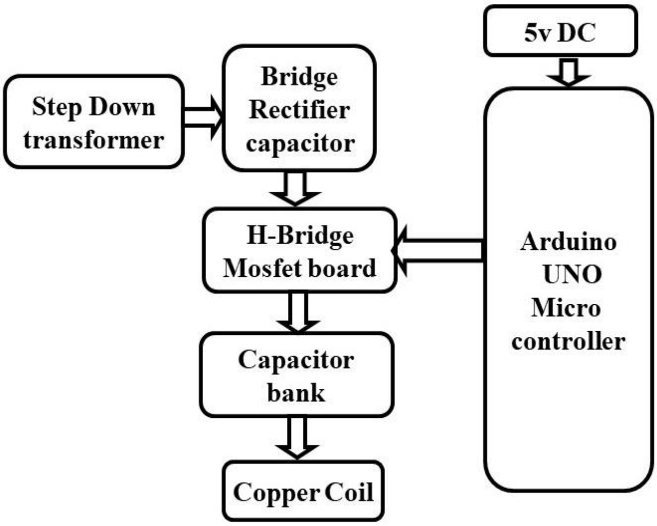

Fig. 1. Wireless charging system for electric vehicle (Transmission Section)

The above block diagram gives the information of primary circuit of system that has components of step-down transformer for varying voltage levels, rectifier for conversion, copper coils for induction of emf

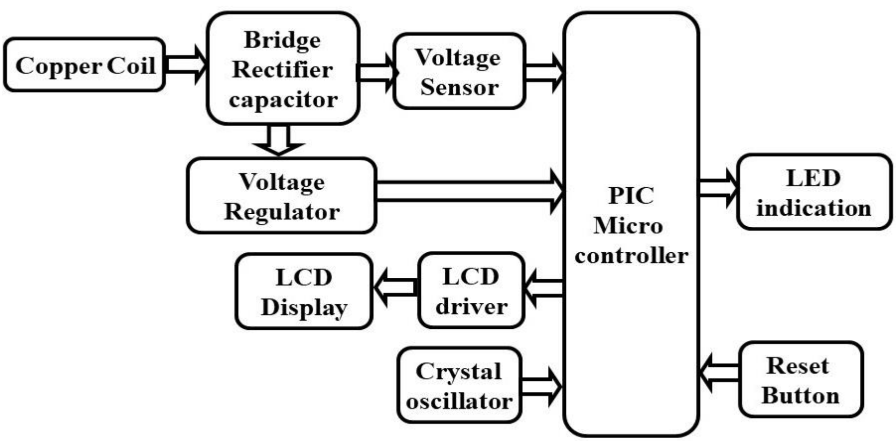

Fig. 2. Wireless charging system for electric vehicle (Receiving Section)

Above fig 2 is the secondary circuit that is incorporated in the E-scooter that receives power by induction process from primary circuit. The receiver circuit consists of the battery connected to the E-Scooter. But, here in prototype, Voltage sensor is kept knowing the voltage induced from the WPT. Various experimental calculations are done for the coil design. For that chosen Battery = 48V ,17.5A, 840W, Supply voltage = 240 V, them 200 Stands 38AWG with Qs (quality factor) =4 and K=0.2 are used.

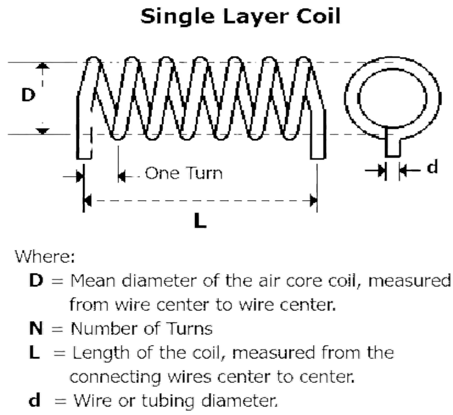

Fig. 3. Topology of single layer Coil

R load (Rl) = $\frac{Vs^2}{Po}$ =2.74 Ω

Secondary Current (Is) = $\frac{Vs}{Rl}$=17.50 A

Primary Current (Ip) = $\frac{Po}{Vs} = 3.5\ A$

Secondary Inductance (Ls) = $\frac{Qs*Rl}{\Omega}$ = 20.536 uH

Mutual Inductance (M) = $\frac{Is*Rl}{Ip*\Omega}$ = 25.678 uH

Primary Inductance (Lp) = $\frac{M^2}{Ls*K^2}$ = 802.421 uH

Coil Inductance:

$$L(uH) = \frac{D^2 * N^2}{18*D+14*L}$$

3.1 Primary coil:

From the given inductance formula,
Obtained results are,
Coil diameter = 135mm
Coil length = 45mm
Number of turns = 66
diameter = 1.2mm
$Area = \pi r^2$ = 1.130mm^2
Current density = $\frac{current}{area}$ = 3.1amp^2
Length = 2πr*(no. of turns) = 2799.15cm.

3.2 Secondary Coil

From the given inductance formula,
Obtained results are,
Coil diameter = 135mm
Coil length = 35mm

Number of turns = 11
Wire diameter = 3mm
$Area = \pi r^2 = 7mm^2$
Current density = $\frac{current}{area}$ = $2.5amp^2$
Length = 2πr*(no. of turns) = 466.52

Thus, the calculation for the primary and secondary coil are done using the required battery specifications. The general circuit schematics are run and created for both system i.e. Transmission and receiving

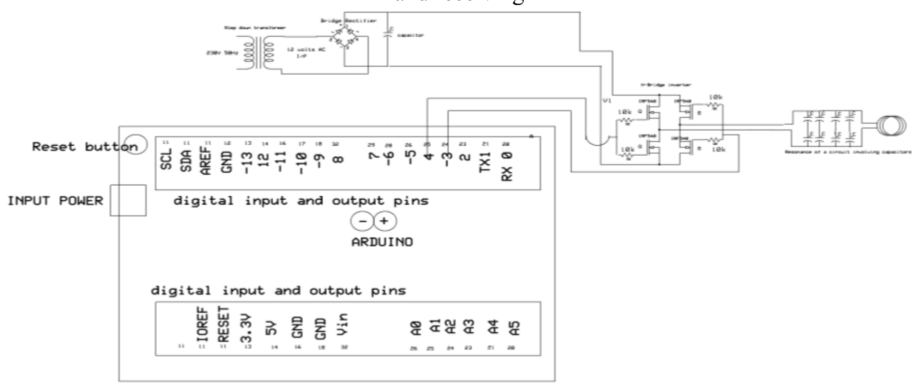

Fig. 4. Schematic circuit diagram with Arduino UNO of the primary side of WPT

The pin diagram of Arduino and its connections along with the MOSFETs are in Fig 4. The required clock pulses to FETs are generated from this Arduino circuit and FETs are functioned based on the input clock pulses.

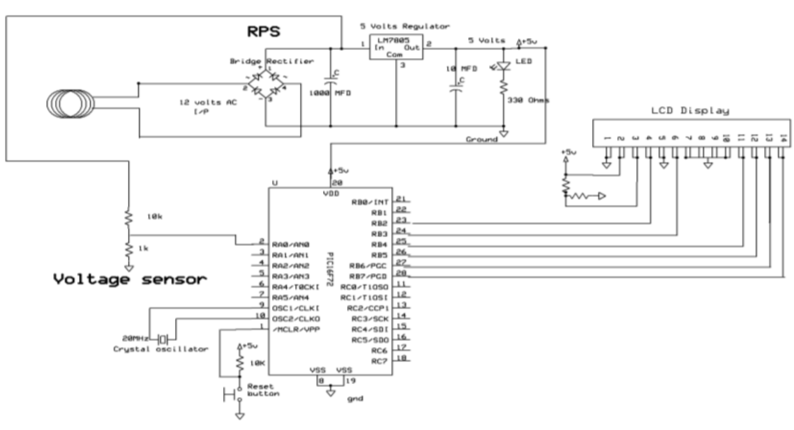

Fig. 5. Schematic circuit diagram of PIC microcontroller with LCD on secondary side

The pin diagram of the microcontroller with LCD along with the connections is in Fig 5 it has a voltage sensor that senses the voltage at the receiving side circuit and displays the value on the LCD digitally.

4 Hardware implementation & Experimental outcomes

The designed circuit i.e. schematic as shown in previous fig 5 &6 are built as hardware model prototype. The images of prototype design that contains all the components that are discussed in hardware requirements.

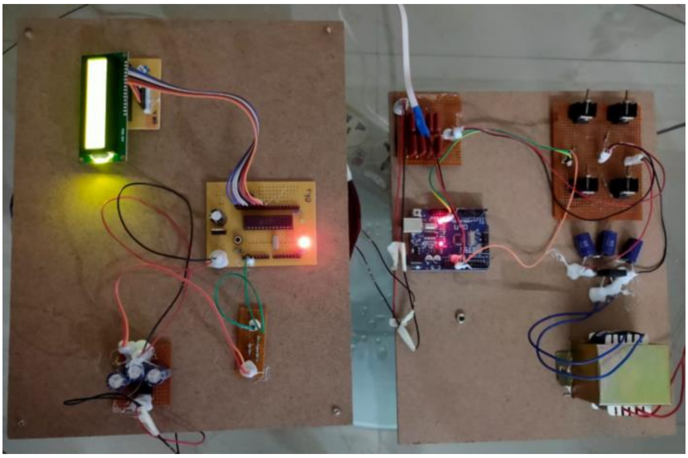

Fig 6(a). Top view of Hardware circuit

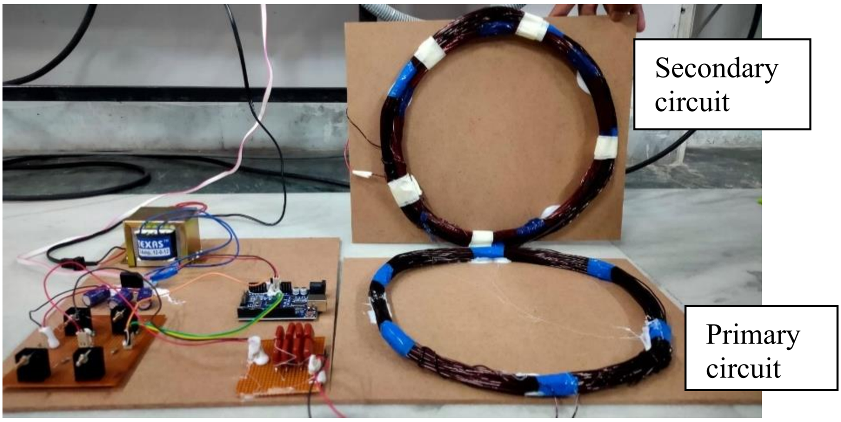

Fig. 6(b). Primary and secondary circuits

From Fig 6(a) top view of the circuit can be observed it contain components like LCD, MOSFETs, Transformer and from Fig 6(b) both primary and secondary circuit can be observed that contains different coil turns. There is no connection between the primary circuit and secondary circuit. Air acts as a dielectric medium of the transfer neglecting some losses, experimentation is carried out.

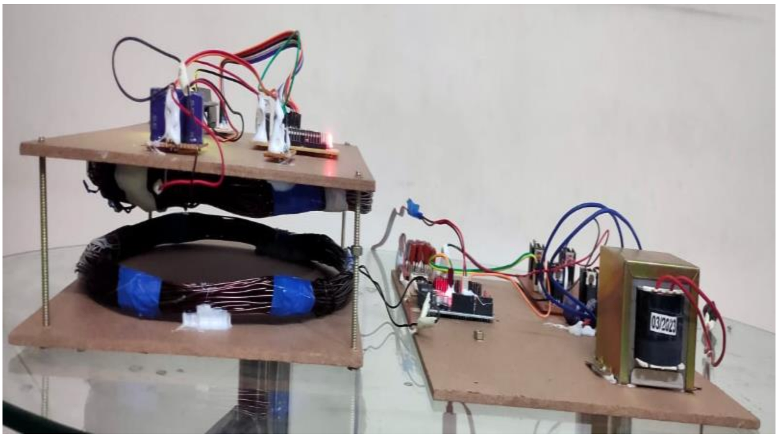

Fig. 7(a). Realtime working model of wireless charging system for electric vehicle

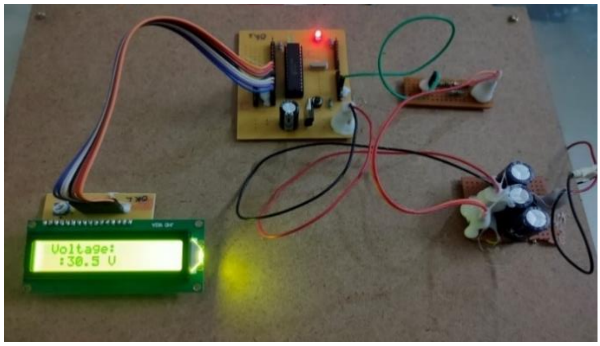

Fig. 7(b). Output of Receiving coil voltage

Primary and secondary circuits are defined in the above images. we can observe that there is a minimum distance from each circuit and LCD is having some voltage values during working condition it shows the output of Voltage sensor that induces in the secondary circuit from fig 7(a) Realtime working model and wireless charging system can be observed completely. It is having all the setup of hardware and from Fig 7(b) induced voltage at receiving circuit can be observed by LCD in digitally with units

Table 1. Distance Vs Induced Voltage

Distance between the coils	Induced voltage at the receiving end (output voltage)
1cm	48.5V
2cm	45V
3cm	41V
4cm	38V
5cm	35V
6cm	33.5V
7cm	30V

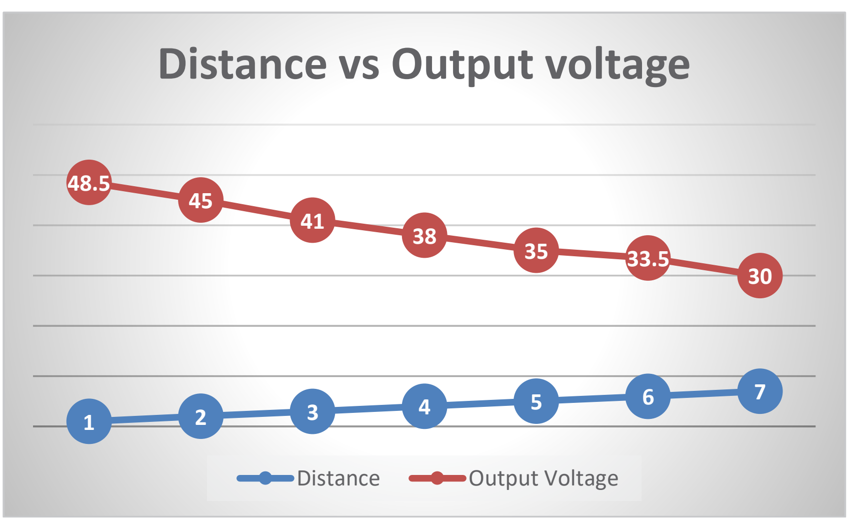

Fig. 8. Plot between distance and induced voltage

Observing from Table 1 and conclude that induce voltage at the receiving end coil will be more when distance is less and vice-versa. When the distance is less i.e., 1cm maximum voltage is induced in the secondary circuit that is 48.5V and when distance is 7cm the induced voltage is minimum of 30V.The variations are clearly interpreted as graph as shown in Fig 8

5 Conclusion

In this paper an attempt to charge an EV vehicle of 48V 17.5AH battery specifications. Where the software analysis was carried out to design the inductance using ANSYS software. The with the designed values hardware prototype implemented for charging the battery. With the work that is carried out a sustainable operation is achieved. The WPT analysis carried out with the distance Vs the induced voltage where the reliability is achieved.

References

1. Mohammad Shahjalal, Tamanna Shams, Mohammed Nishat Tasmin, Md Rishad Ahmed, Mominul Ahsan, and Julfikar Haider, Charging Tech. (2020).
2. J. Li, E. Murphy, J. Winnick, P. A. Kohl, J. Power Sources (2001).
3. Mohamed Y. Metwly, Mahmoud S. Abdel-Majeed, Ayman S. Abdel-Khalik, Ragi A. Hamdy, Mostafa S. Hamad, Shehab Ahmed, Electronics, (2020).
4. Murat Yilmaz, Philip T. Krein, IEEE EV Conf. (2012)
5. Awaar, Vinay Kumar, Praveen Jugge, S. Tara Kalyani, and Mohsen Eskandari *Dynamic "Voltage Restorer–A Custom Power Device for Power Quality Improvement in Electrical Distribution Systems",* In Power Quality: Infrastructures and Control, pp. 97-116. Singapore:Springer Nature Singapore, (2023).
6. SAE Electric Vehicle and Plug-in Hybrid Electric Vehicle Conductive Charge Coupler, SAE J1772, Jan (2010).
7. Yadasu, Shyam, Vatsala Rani Jetti, Vinay Kumar Awaar, and Mohan Gorle. "*Development of Novel Pulse Charger for Next-Generation Batteries."* Energy Technology 11, no. **3** (2023).
8. Awaar, V.K., Jugge, P. & Tara Kalyani, *"Validation of Control Platform Using TMS320F28027F for Dynamic Voltage Restorer to Improve Power Quality",* S. Journal of Control Automation and Electrical Systems, **30**, no.4, pp 601-610, (2019).
9. Karthik Rao, R., Bobba, P.B., Suresh Kumar, T., Kosaraju, S. *"Feasibility analysis of different conducting and insulation materials used in laminated busbars"* Materials Today: Proceedings, 26, pp. 3085-3089, (2019).
10. Tummala, S.K., Bobba, P.B., Satyanarayana, K. "*SEM & EDAX analysis of super capacitor"*, Advances in Materials and Processing Technologies, 8 (sup4), pp. 2398-2409, (2022).
11. Tummala, S.K., Kosaraju, S. *SEM analysis of grid elements in mono-crystalline and poly-crystalline based solar cell* Materials Today: Proceedings, 26, pp. 3228-3233, (2019).
12. Mohamed Aboualalaa, Islam Mansour, Ramesh K.Pokharel Experimental study of effectiveness of metasurface for efficiency and misalignment enhancement of Near-Fied WPT system IEEE Antennas And Wireless Propagation Letters, 21,10, (2022).
13. Y Yao & W Zhong General Model and analysis of misalignment characteristics of fixed-frequency WPT system IEEE Transc. Power Electronics, 38, 11, (2023).
14. Y Fei, F Chen, R Gao, S Zhao, Chunsen Tang, Lei Zhao "Oscillation frequency manipulation in autonomous WPT systems with series-series compensation" IEEE transc. 39, 1, (2024)